

Experimental investigation of performance of microchannel condenser with effect of air velocity for personal cooling system for firefighters

Satheesh Kumar Sankar^{a,*}, Kumaraguruparan Gurusamy^b & Balachandran Natarajan^c

^aDepartment of Mechanical Engineering, M.Kumarasamy College of Engineering, Karur, Tamil Nadu 639 113, India

^bDepartment of Mechatronics Engineering, Thiagarajar College of Engineering, Madurai, Tamil Nadu 625 015, India

^cCold Storage Consultant, Madurai, Tamil Nadu, 625 018, India

Received: 24 June 2024; accepted: 17 December 2024

Personal cooling systems (PCS) have been developed because they have reduced heat stress and heat-related injuries. PCS performance has depended on environmental factors, namely ambient temperature, air velocity, intensity level, and humidity. Among these factors, air velocity has had the potential to cause improper air distribution over the tube bundles of air-cooled condensers, exhaust air recirculation, and poor fan performance. Hence, our goal has been to experimentally investigate the performance of PCS using two microchannel condensers (MCC-1 and MCC-2) under the effect of air velocity (1.5–8.5 m/s). PCS performance has been determined by cooling capacity, COP, and reversible efficiency. These metrics have increased as air velocity and heat input have increased. At the air velocity of 8.5 m/s (maximum), the cooling capacity, COP, and reversible efficiency of MCC-1 have been 0.2%, 2.4%, and 12.62% more than MCC-2 for 100 W. Similarly, at the same air velocity (8.5 m/s), the cooling capacity, COP, and reversible efficiency of MCC-1 have been 3.2%, 0.2%, and 13.1% more than MCC-2 for 500 W. Results have shown that the change in cooling capacity and COP of MCC-1 and MCC-2 has remained just under 3.2%. Hence, it has been concluded that MCC-1 and MCC-2 have performed similarly at all air velocities. However, based on condenser size and weight, MCC-2 has been preferred for the development of a PCS.

Keywords: Air velocity, Firefighters, Microchannel condensers, Mini vapor compression refrigeration system, Personal cooling system

1 Introduction

Thermal comfort is an important role in the textile industry. Because, cloth is to be direct contact with human body. The body temperature will be increased when the workers are performing their strenuous physical activities, industrial activities, or carry out military operations in hot environment conditions while wearing thick and heavy vests. Furthermore, firefighters are performing rescue operations in a hot and hostile environment for an undetermined amount of time¹⁻⁶. The multiple factors can affect the firefighter's physiological responses and it results, including (i) working muscles generate metabolic heat, (ii) heavy, thick, impermeable protective clothing that raises metabolic work rate and, in exceptional situations, (iii) the heat from the fire's radiant sources⁷. In order improve the physiological responses of the firefighters, Individual cooling systems must be used, and work is being done to create an effective individual cooling system⁸. The best personal cooling system should be based on

water cooled, air cooled and phase changing material (PCM) with protective clothing in hot environmental conditions.

Billingham invented the concept of liquid cooling garments (LCG) in the 1950s, and the first LCG is produced by Burton and Collier from the Royal Aviation Institute in the 1960s⁹. Because of high reliability and cooling efficiency, it is used widely in cooling technology compared to other cooling methods namely air cooling and PCM¹⁰⁻¹². Water's high heat capacity benefits from reduced pumping power and system weight. LCGs are thus widely used in both civilian and military applications. LCGs that use ice as a cooling source, on the other hand, have been shown to be highly efficient and cost-effective. As a result, in today's applications, this type of cooling jacket is the most widely used active cooling garment¹³. Also, LCGs that use thermoelectric cooler and vapor compression refrigeration (VCR) system as a cooling source. The Peltier effect is used by thermoelectric cooling systems to transfer the heat from the cold end to the hot end whenever a voltage is applied. A thermoelectric cooling technology is

*Corresponding author (E-mail: sateeskanna@gmail.com)

appealing because it is better suited for small capacity applications such as chip cooling, water heating and cooling, and building space cooling¹⁴. VCR system mainly comprises of compressor, condenser, expansion valve and evaporator. Compressor requires the electrical power. Vapor compression refrigeration (VCR) cooling systems offer a higher coefficient of performance (COP) compared to thermoelectric cooling, making them more efficient. Miniaturizing VCR systems is advantageous due to their (i) simple in construction; (ii) compactness (i.e., lightweight and small footprint); (iii) fewer moving parts; (iv) less maintenance; and (v) reasonably efficient compared to other technologies¹⁵⁻²⁰.

Based on these advantages of VCR system, personal cooling vests are developed from 1990s. First, US army developed R134a based VCR-based PCS for M9 Armored Combat Earthmover (ACE) in 1990s. It is called STEPO microclimate cooling system. At an atmosphere temperature of 35°C, the VCR system has a cooling capacity of 280 W. A total weight of the system is 13.6 kg, including the garment²¹. Wu *et al.*²² established a 2.85 kg miniature vapor compression-based refrigeration (MVCR) system for microclimate cooling. The entire MVCR system consumes a mass of 4 kg, which includes the lithium-ion battery. The system features with overall dimensions of 260 x 250 x 120 mm³, a cooling capacity of 300 W, and a COP of 2.0. A prototype was developed VCR based PCS for car racing pilots²³. With an ambient temperature range of 35°C -45°C, they studied in real-time environmental conditions. They successfully developed a 3.5 kg personal cooling system that delivered a 134 W cooling capacity. This performance was observed with a jacket entry water temperature of 17.3°C and under ambient temperatures of 35°C, 45°C, and 60°C.

VCR-based man-mounted cooling system was created²⁴. The cooling capacity of 57 W is obtained at an ambient temperature of 35°C. The entire system weight is 2.2 kg, including the battery. It operates for 6 hours on a single battery. Ernst and Garimella²⁵ developed a wearable PCS based on the VCR system for firefighter, military and chemical response duty personnel applications. The test is conducted for the heat removal range from 100 to 300 W for the range of an ambient temperature of 37.7°C - 47.5°C. The total mass of the wearable PCS is 5.31 kg, and it gives a cooling capacity of 178 W at an ambient temperature of 43.3°C for 5.7 hours. Guo²⁶ designed and developed a liquid-based cooling system for hot

environmental conditions. They analyzed in all real-time hot environmental situations using a thermal manikin. They found that an ambient temperature would significantly affect the liquid-based cooling system's work duration time.

Yuan *et al.*²⁷ constructed a VCR-based portable personal cooling system by the indirect cooling method. The system's total mass is 5.25 kg, including a battery and a cooling vest. At an ambient temperature of 50°C and the cold-water temperature of 24°C, the system cooling capacity of 260 W is obtained for to cool a person sufficiently with a medium workload at a hot environment and produces a COP of 1.62. Dabrowska *et al.*²⁸ designed an active LCG for hot environmental conditions. The cooling system, which weighs less than 10 kg, provided a 300 W cooling capacity at a mass flow rate of 3.8 l/min. Climatic chamber tests under varying atmospheric conditions (30°C - 45°C air temperature, 20%–80% relative humidity, 0.4 m/s air velocity) showed the designed LCG system's efficiency in hot environments. Kumar and Kumaraguruparan²⁰ developed the personal cooling system for firefighters under moderate working conditions (ambient temperature range: 34–50 °C and heat generation range: 100–500 W). They used Aspen miniature compressor, multilouver microchannel condenser, capillary tube and flexible tube evaporator. It is direct cooling method. They are eliminated the secondary cooling medium loop. They investigated the cooling system with effect of two condensers and capillary tubes. They found that the 1.18 mm ID capillary tube with MC-2 performed better than others for its high COP and cooling capacity. They develop the cooling system with weight of 4.335 kg including battery.

Condenser performance was analyzed by the heat transfer rate from the condenser. This performance of the condenser depends on the air velocity and refrigerant circuit configuration. Lee and Jeong²⁹ investigated the condenser performance with effect of non-uniform distributions of the air flow. They concluded that, heat transfer performance is drastically reduced depending the air velocity, air flow and refrigeration circuit configuration. Yang *et al.* (2011)³⁰ performed the thermal performance of air-cooled condenser with effect of ambient wind. Ambient winds have the potential to cause improper air distribution over the tube bundles of the air-cooled condensers, recirculation of exhaust air, and subpar fan performance. Louvered finned type condensers were investigated related to its geometrical

parameters and flow parameters on heat transfer and pressure drop characteristics. They reported detailed review of various louvered finned type condenser on its performance with effect flow and geometrical parameters³¹. Then, Louvered finned condenser was investigated with effect of Vortex Generators (VGs) on heat transfer enhancement by many investigators by varying geometrical parameters like shape, location, attack angle, aspect ratio, and Reynolds number (Re)³². Meikandan *et al.*³³ investigated the bare helical tube cross flow heat exchangers performance by experimental and numerical method. COMSOL was used for numerical analysis. They performed the work for 16 different sets of heat exchangers with air velocity range of 0.5 -1.5 m/s. They found a good agreement between the numerical and experimental findings with a maximum error of 0.3%. Many researchers^{34,35} investigated the condenser performance with effect of wind and non-uniformity of the air flow for various applications such as space, power plants and automobile sectors. They are concluded that, still air-cooled condenser has to be investigated for the wind speed and to obtain the uniform air flow for respective applications.

From the reviewed literature study shows that the miniaturization of VCR system is possible and it uses for personal cooling system. Also, it shows that the efforts are to be taken to designing a PCS for better performance with accounting the performance parameters of refrigerant mass flow rate, suction pressure, evaporator temperature and ambient temperature. But, the external factors namely, air velocity, intensity level, humidity and weight of the system are also affecting the performance of the PCS. Hence, the goal of this work is to examine the performance of PCS for firefighters using two different sizes of microchannel condensers (MCC-1 and MCC-2) with the effect of air velocity (range: 1.5-8.5 m/s) under moderate environmental conditions. Based on a metabolic heat generation range of

100-500 W and a maximum ambient temperature of 50°C, this analysis selects the superior-performing multilouvered condenser for use with the small-scale personal cooling system.

2 Materials and Methods

2.1 Experimental set-up

The VCR-based personal cooling system incorporates four basic components. To begin, system evacuation is done by the vacuum pump (Model: REFCO RL-8-RS). The R134a is then charged and the required amount of refrigerant is filled using a digital manifold (Model: Testo 570-1) and a programmable charging scale (Model: REFCO REF-METER-OCTA-KIT). Pressure and temperature sensors are fitted at the inlets and outlets of the compressor, condenser, capillary tube, and evaporator to record refrigerant pressure and temperature with an accuracy of ± 0.01 bar and $\pm 0.1^\circ\text{C}$, respectively. Refrigerant thermal mass flow sensor (Model: Compact regulator GCR-D9KA-BA30) with an accuracy of $\pm 2.0\%$ end value, is used to measure the mass flow rate of refrigerant. The K-thermocouples are used to measure water temperature with an accuracy of $\pm 1^\circ\text{C}$ and the surface temperature of the flexible tube. Table 1 lists the equipment specifications.

A picture of experimental setup is shown in Fig. 1. A flowing water pump circuit provides heat equivalent to that of the human body. A water mass flow meter, a water heater, a waterpump, and hoses are all part of this loop. The flexible evaporator tube (on the R134a side) is immersed in water. The water tank holds 10 litres of water. The water is circulated by a water pump, and a control valve is placed at the pump outlet. The mass flow rate of water is maintained by the control valve and measured by a Rotameter (Make: Bellstone) with a measurement range of 0-5 L/min and an accuracy of 2% full scale. In this work, the mass flow rate of water is kept constant at 3 L/min. To measure water temperatures,

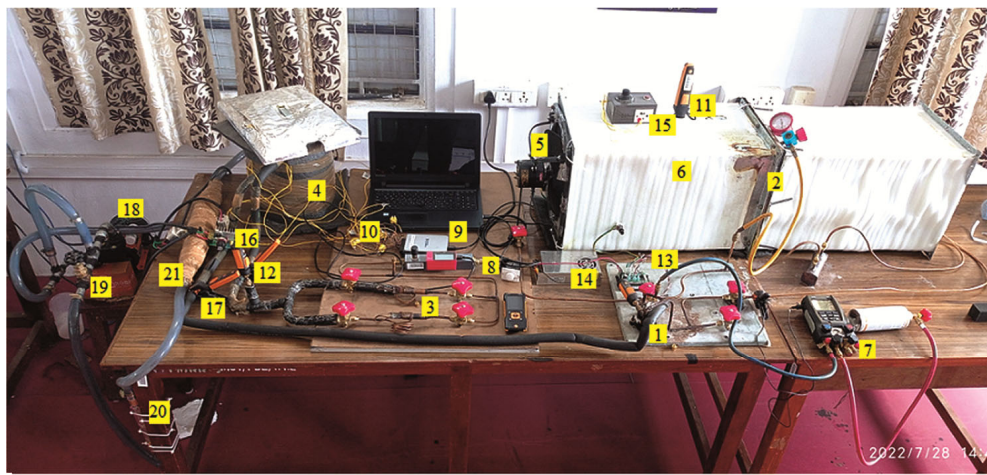
Table 1 — Details of equipment used.

Measurement	Brand/Model	Measuring range	Precision/error
Refrigerant temperature sensor	Testo	-40 to +150°C	$\pm 0.1^\circ\text{C}$
Refrigerant pressure sensor	Testo	-1 to 60 bar	0.01 bar
Refrigerant mass flow sensor	Vogtlin	4.4-220 g/min	$\pm 2.0\%$ end value
Thermocouple	K type	-50-200°C	$\pm 1^\circ\text{C}$
Clamp meter	Testo	1 mV - 600 V AC/DC 0.1 - 600 A AC/DC	--
Vane probe ($\phi 16\text{mm}$)	Testo	0.6 to 50 m/s	± 0.1 m/s
Differential pressure sensor	Testo	-150 to +150 hPa	± 0.2 hPa
Water mass flow meter (Rotameter)	Bellstone	0 to 5 L/min	0.01 L/min

thermocouples are placed at the entrance and exit of the water tank, as well as the entry and exit of the water heater. The water heater is connected to a variable transformer to provide the necessary heat input, which is measured using a Testo clamp meter (Model: Testo 770-3). Polyethylene foam insulates the water tank, providing a thermal barrier between the tank and the surrounding environment.

Figure 2(a) depicts the schematic diagram of the small VCR-based personal cooling system. As R134a travels through the evaporator, heat is absorbed by the low-pressure liquid refrigerant.

When the superheated vapor reaches the compressor, its pressure is increased. Because some of the energy used in the compression process is passed to the refrigerant, the temperature will also increase. The compressor sends high-pressure superheated gas into the condenser. The gas is first cooled to a lower temperature in order to transform it back into a liquid. In order to reduce temperature during this procedure, air is typically used. The expansion device regulates the flow into the evaporator and lowers the pressure of the high-pressure sub-cooled liquid, preparing it for the



- | | | |
|--|--|------------------------------------|
| 1. Miniature Rotary Compressor | 8. Refrigerant Mass flow mater | 15. Air Heat Controller |
| 2. Multilouvered Microchannel Condenser | 9. Data acquisition system with computer | 16. Evaporator Heater Controller |
| 3. Capillary Tube | 10. K - type Thermocouples | 17. Refrigerant Temperature sensor |
| 4. Water tank (Evaporator - flexible tube) | 11. CO ₂ sensor for Temperature measurement | 18. Motor pump (Water Circulation) |
| 5. Condenser fan | 12. Refrigerant Pressure sensor | 19. Throttle valve |
| 6. Wind tunnel setup | 13. Microcontroller board for rotary compressor | 20. Rotameter |
| 7. Digital Manifold | 14. SMPS | 21. Water heater |

Fig. 1 — Experimental setup of VCR-based personal cooling system.

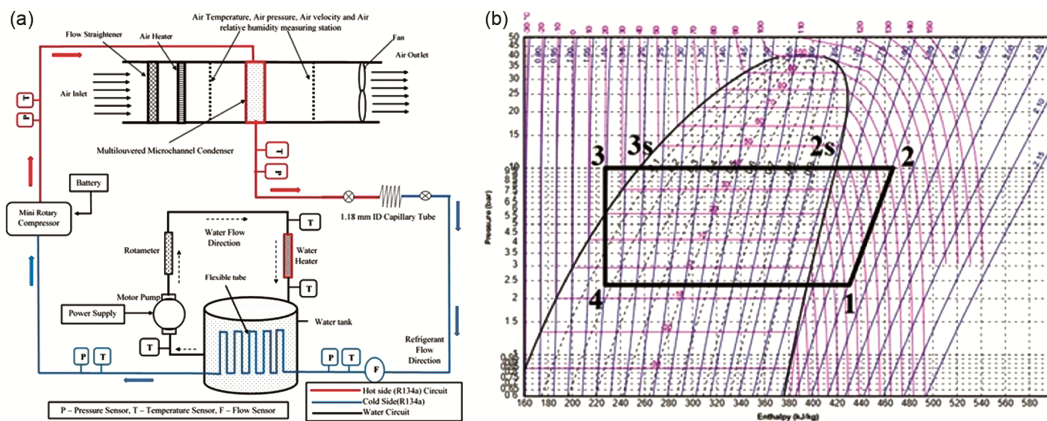


Fig. 2 — Details of the miniature VCR-based personal cooling system (a) Schematic diagram, and (b) pressure-enthalpy diagram of the R134a.

subsequent cycle. The important refrigeration cycle is illustrated in the pressure-enthalpy diagram (Fig. 2 (b)).

A wind tunnel was built to study airflow uniformity and the airside performance of microchannel condensers at different air temperatures. A heating device in the wind tunnel is used to achieve the desired air temperature at the inlet. To achieve the appropriate inlet air temperature, the variable transformer is employed to alter the air heater load. The entry and exit air temperatures of the microchannel condenser are measured using thermocouples with $\pm 1^\circ\text{C}$ precision. The airside velocity is measured with an accuracy of ± 0.1 m/s using a 16 mm diameter vane probe (Make: Testo). An IAQ measuring equipment with an integrated differential pressure sensor with an accuracy of 0.2 hPa is used to monitor the airside pressure drop. The polyethylene foam insulates the wind tunnel's outer surface and functions as a thermal barrier between the system and its surroundings.

2.2 Test section - Microchannel condenser

In this work, two multilouvered microchannel condensers are investigated for the better performance of the personal cooling system. The schematic diagrams of these two condensers are shown in Fig. 3. The geometry details of these two condensers are listed in Table 2.

2.3 Data reduction and method

2.3.1 Refrigerant side performance

The coefficient of performance (COP), cooling capacity, and reversible efficiency of a small VCR-based personal cooling system are utilized to assess its effectiveness. The formulas are given below:

Evaporator load (Q_E)

$$Q_E = M_R \times (h_1 - h_4) \quad \dots (1)$$

Where M_R represents the refrigerant mass flow rate (kg/s), h_1 and h_4 represent the enthalpy at outlet and inlet of an evaporator (kJ/kg).

Heat rejection rate (Q_C)

$$Q_C = M_R \times (h_2 - h_3) \quad \dots (2)$$

Where h_2 and h_3 are the condenser enthalpies at the inlet and output, respectively.

Work input required to run the compressor (W_{in})

$$W_{in} = M_R \times (h_2 - h_1) \quad \dots (3)$$

Where, h_1 and h_2 are the compressor's enthalpy at the inlet and outlet (kJ/kg).

Degree of subcooling temperature (ΔT_{Sub})

$$\Delta T_{Sub} = T_{sat @ P_3} - T_3 \quad \dots (4)$$

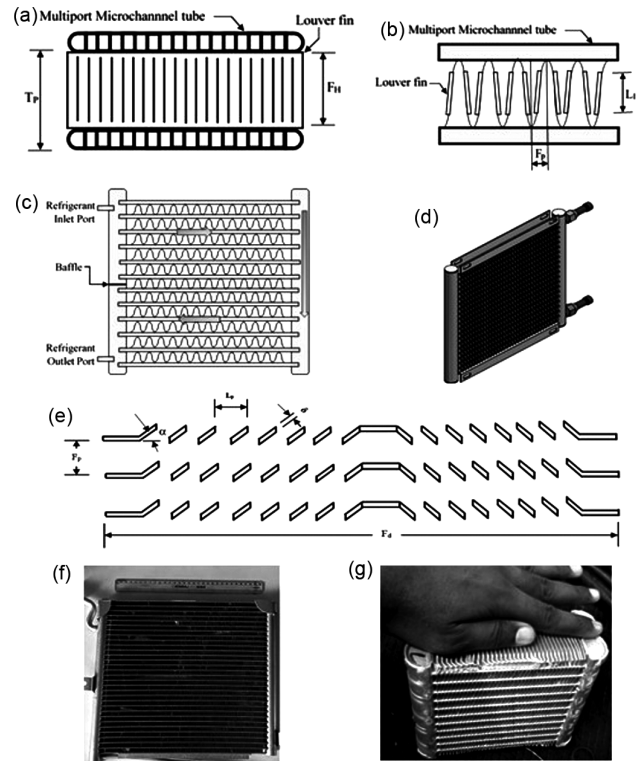


Fig. 3 — Schematic representation of multilouvered microchannel condenser (a) Microchannel geometry, (b) Louver geometry, (c) Front face view, (d) CAD model, (e) Louver arrangement, (f) Microchannel condenser (MC-1) picture, and (g) Microchannel condenser (MC-2) picture.

Table 2 — Condenser geometry details.

Type and geometry parameter	Multilouvered microchannel condenser	
	MCC-1	MCC-2
Width (W)	360 mm	200
Height (H)	320 mm	180
Depth (d)	18 mm	32
Hydraulic diameter (D_H)	0.776	1
Channel width (w_c)	0.6 mm	0.75
Channel height (h)	1.1 mm	1.5
Wall thickness (w_t)	0.45 mm	0.5
Channel length (l)	336 mm	178
Number of channels	18	21
Fin pitch (F_p)	1 mm	1.4
Fin height (F_H)	8 mm	12.5
Fin thickness (δ)	0.1 mm	0.1
Tube thickness (t)	2 mm	2.5
Tube pitch (T_p)	10 mm	15
No of tubes	29	11
Louver pitch (L_p)	1 mm	1
Louver angle (α)	18°	20°
Louver length (L_L)	6 mm	9

Where, P_3 , T_3 is the outlet pressure and temperature outlet at the condenser, respectively, and T_{sat} is the saturation temperature.

Degree of superheating temperature (ΔT_{Sup})

$$\Delta T_{Sup} = T_1 - T_{sat @ P_1} \quad \dots (5)$$

Where, P_1 , T_1 is pressure outlet and temperature outlet at an evaporator, respectively.

COP is defined as the ratio between the system cooling load and the work input to run the compressor. It is given below:

$$COP = \frac{Q_E}{W_{in}} \quad \dots (6)$$

Equation 7 determines the volumetric efficiency of the compressor.

$$\eta_v = \frac{M_R}{(n/60) \times \rho_{in} \times V_{dis}} \quad \dots (7)$$

Where n is compressor speed (rpm), ρ_{in} is the density of the refrigerant (kg/m^3) at the compressor inlet, V_{dis} is the rotary compressor displacement volume in m^3 ($V_{dis} = 1.9e^{-6} \text{m}^3$) and η_v is the compressor volumetric efficiency.

Reversible efficiency (η_{rev}) is determined using Eq. 8.

$$\eta_{rev} = \frac{COP}{COP_{rev}} \quad \dots (8)$$

Where, COP_{rev} is the reversible COP calculated by the Carnot cycle utilizing condenser and evaporator temperatures.

$$COP_{rev} = \frac{1}{(T_c/T_e) - 1} \quad \dots (9)$$

Where, T_c is condenser temperature and T_e is the evaporator temperature.

2.3.2 Air side performance

According to energy balance in vapor compression refrigeration system³⁶.

$$Q_a = \varepsilon Q_c \quad \dots (10)$$

Where, ε is thermal leakage factor (0.971).

Airside heat transfer rate

$$Q_a = m_a c_{p,a} (T_{a,out} - T_{a,in}) \quad \dots (11)$$

Refrigerant side or Condenser heat transfer rate

$$Q_c = M_R (h_2 - h_3) \quad \dots (12)$$

Heat transfer capacity from the condenser

$$Q = \frac{1}{2} (Q_a + Q_c) \quad \dots (13)$$

Overall thermal conductance

$$UA = \frac{Q}{F \Delta T_{lm}} \quad \dots (14)$$

Log Mean Temperature Difference (LMTD)

$$LMTD (\Delta T_{lm}) = \frac{[(T_{r,out} - T_{a,in}) - (T_{r,in} - T_{a,out})]}{\ln[(T_{r,out} - T_{a,in}) / (T_{r,in} - T_{a,out})]} \quad \dots (15)$$

Fin efficiency

$$\frac{1}{\eta_o h_o A_o} = \frac{1}{UA} - \frac{1}{h_i A_i} - \frac{\delta_w}{k_w A_w} \quad \dots (16)$$

$$h_i = \frac{Q}{\pi D_H L (T_s - T_w)} \quad \dots (17)$$

$$\eta_o = 1 - \frac{A_f}{A_o} (1 - \eta_f) \quad \dots (18)$$

$$\eta_f = \frac{\tanh(ml)}{ml} \quad \dots (19)$$

$$\text{Where, } m = \sqrt{\frac{2h_o}{k_f \delta_f}}, l = \frac{H_f}{2}$$

where T_s is the refrigerant saturation temperature, T_w is the tube wall temperature, D_H is the hydraulic diameter, and L is the tube length. Also, η_f denotes the louver fin efficiency, δ_f denotes the thickness of the louver fin, and δ_w denotes the wall thickness of the microchannel tube.

Colburn-j factor

$$j = \frac{h}{c_{p,a} G_a} Pr_a^{2/3} \quad \dots (20)$$

$$\text{Where, } G_a = \frac{\dot{V}_a \rho_a}{A_{fr}} \quad \dots (21)$$

where A_{fr} denotes the free-flowing area in the microchannel condenser and A_o denotes the total heat transfer area of the microchannel condenser.

Fanning friction factor

$$f = \left(\frac{A_{min}}{A_o} \right) \left(\frac{\rho_a}{\rho_{a,in}} \right) \left\{ \frac{2 \Delta P_a \rho_{a,in}}{G_a^2} - \left(\frac{\rho_{a,in}}{\rho_{a,out}} - 1 \right) (1 - \sigma^2) \right\} \quad \dots (22)$$

$$\text{Where, } \sigma = \frac{A_{fr}}{A_{fa}}$$

where $\rho_{a,in}$ and $\rho_{a,out}$ are the air inlet density and air outlet density respectively and ρ_a is the average of the air densities at the inlet and outlet sections and σ denotes the ratio of the free-flowing area to frontal area of the microchannel condenser.

2.3.3 Method and operating conditions

Two multilouvered microchannel condensers (MCC-1 and MCC-2) were analyzed using Wind tunnel arrangement with the air velocity range of

1.5–8.5 m/s on moderate environmental conditions for firefighters (Metabolic heat generation rate = 100–500W and maximum ambient temperature = 50°C). The metabolic heat is given as evaporator heat load and five intervals is taken for this work with the interval size of 100. The performance of the MCC-1 and MCC-2 condensers are performed with the effect of air velocities for different evaporator load conditions.

3 Results and Discussion

3.1 Effect of air velocities and heat inputs on PCS performance

Miniature VCR-based PCS system performance is evaluated using the following parameters namely, cooling load capacity, COP, and the reversible efficiency. These variations are shown in Figs (5-7). The parameters of the PCS, namely, $T_a = 50^\circ\text{C}$, $n = 6500$ rpm, $M_R = 95.1$ g/min, $M_W = 3$ L/min and $M=160$ g, are kept constant. The variation of suction pressure with the effect of air velocity is shown in Fig. 4. It displays that the suction pressure declines with a rise in air velocity and increases with a rise in heat input. The suction pressure of MCC-2 is more than that of MCC-1 in all heat inputs. Because two-phase heat transfer performance (condensation of the refrigerant) declines when the air velocity decreases, it will produce a higher exit temperature at condenser outlet and it reflects that higher evaporator pressure in lower air velocity than higher air velocity. It reveals that when decreasing the air velocity, the suction pressure of MCC-1 is increased by 8.57% and 6.4% for 100 W and 500 W respectively. However, MCC-2 is increased by 6.6% and 6.4% for 100 W and 500 W

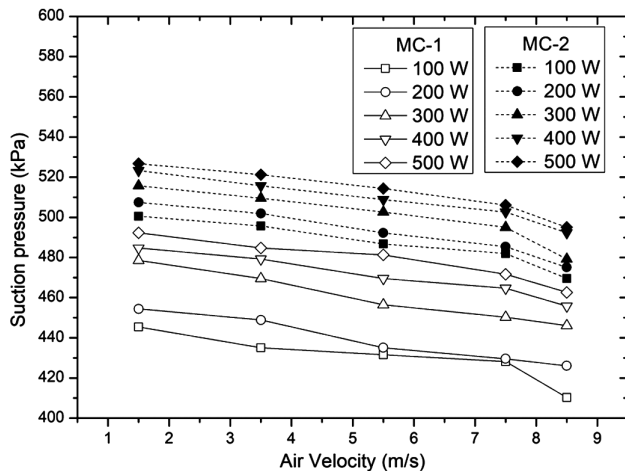


Fig. 4 — Effect of air velocity on the suction pressure for $T_a = 50^\circ\text{C}$, and $n=6500$.

respectively. Hence, it is clearly showing that the increase of suction pressure of MCC-2 is observed for maximum heat inputs while air velocity decreases.

The variation of the cooling capacity under different air velocities and body heat inputs is shown in Fig. 5. It shows that the cooling load capacity rises with a growth in air velocity and heat input. When the air velocity increases, the cooling capacity of MCC-1 is increased more than that of MCC-2. Because the MCC-1 condenser has a larger surface area than MCC-2, results that the two-phase heat transfer performance of MCC-1 is better than MCC-2. Also, the degree of subcooling in MCC-1 is more than that of MCC-2 and it enhances heat transfer performance in the evaporator, increasing the cooling capacity of MCC-1. The average enhancement of the cooling load capacity is 1% and 3% for MCC-1 and MCC-2 in all heat inputs while decreasing the air velocities. At the maximum air velocity (8.5 m/s), the cooling capacity of MC-1 is 0.2% and 3.2% higher than that of MC-2 for 100 W and 500 W. Hence, it concludes that the cooling capacity does not vary too much while increasing the air velocities in both MCC-1 and MCC-2.

The total power consumption by the miniature VCR system is determined by adding the compressor work done by the rotary compressor and electrical work required to drive the fan in the microchannel condenser unit. The compressor work is illustrated in Fig. 6 for MCC-1 and MCC-2 respectively.

This is clearly stated that, the almost same compressor work is required to drive the system with MCC-1 and MCC-2 respectively. The required compressor work is minimum at the maximum air

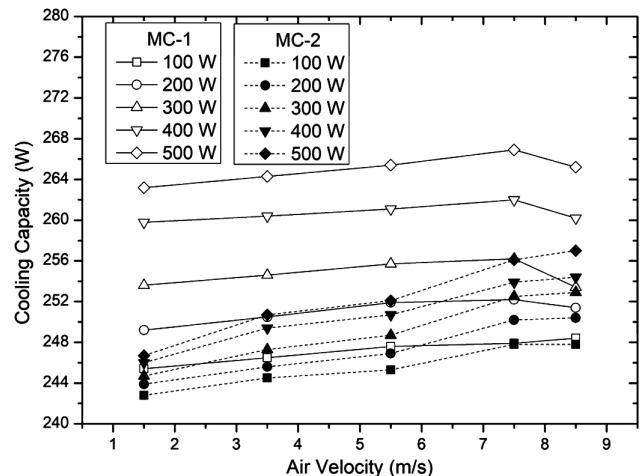


Fig. 5 — Cooling capacity variation under several air velocity and heat input for $T_a = 50^\circ\text{C}$, and $n=6500$.

velocity of 8.5 m/s. Figure 7 shows the system COP variation under several air velocities and body heat inputs. It shows that the COP enhances with a rise in air velocity and body heat input. At 100 W, the increase in COP is 16.22% and 18.5 % for MCC-1 and MCC-2 respectively when air velocity increases. However, at 500 W, the increase in COP is 21% and 21.7% for MCC-1 and MCC-2 respectively. Although, the COP of MCC-1 is more than that of MCC-2 because the mass flow rate of refrigerant of MCC-1 is higher than MCC-2, it results that the cooling capacity of MCC-1 increasing. Also, compressor work is higher in MCC-1. At maximum air velocity (8.5 m/s), the system COP of MCC-1 is 2.4% and 0.2% higher than that of MCC-2 for 100 W and 500 W correspondingly. The change in COP of MCC-1 and MCC-2 is very negligible due to higher

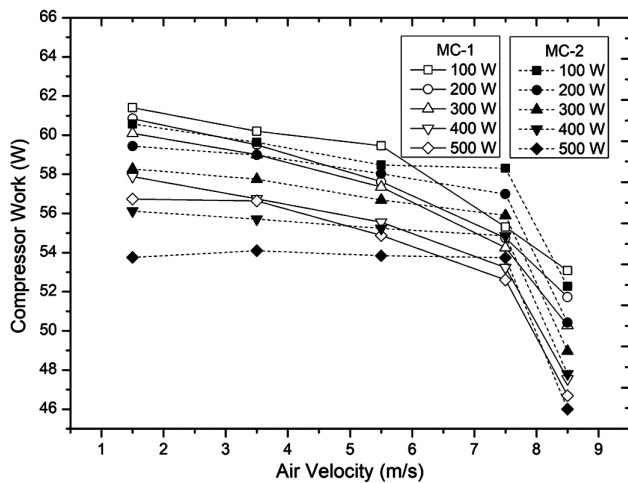


Fig. 6 — Cooling capacity variation under several air velocity and heat input for $T_a = 50^\circ\text{C}$, and $n=6500$.

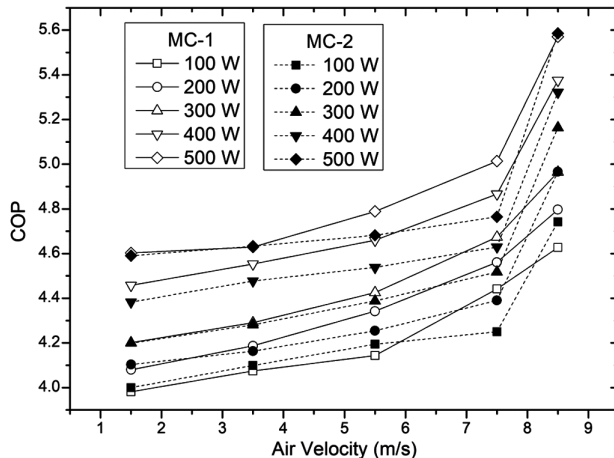


Fig. 7 — Effect of air velocity and heat input on system COP for $T_a = 50^\circ\text{C}$, and $n=6500$.

suction pressure of MCC-2 is more than the MCC-1. As a result, the MCC-1 and MCC-2 functioned identically across all air velocities.

When there is a temperature difference, the capillary tube expands, and the compressor compresses, the irreversible efficiency is demonstrated. Figure 8 shows how reversible efficiency varies with air velocity and heat input. The reversible efficiency, like cooling capacity and COP, improves with increased air velocity and heat input. When ambient and water temperatures are similar, condensation temperature decreases and evaporation temperature rises, minimizing system exergy loss and enhancing reversible efficiency^{37,38}. At 500 W, the increase in reversible efficiency is 23.18% and 24.13% for MCC-1 and MCC-2 while air velocity increases. But, at 100 W, the increase in reversible efficiency is 18.77% and 19.56% for MCC-1 and MCC-2 respectively. However, at 8.5 m/s (maximum air velocity), the increase in reversible efficiency of MCC-1 is 12.62% and 13.1% higher than that of MCC-2 for 100 W and 500 W respectively. MCC-1 has a higher reversible efficiency than MCC-2 because of its high condensation and evaporation temperatures. Furthermore, a large refrigerant charge ($M=160\text{ g}$) results in a high evaporation pressure and reduces the temperature differential in the evaporator during heat transfer.

3.2 Uncertainty analysis

The uncertainty analysis procedure of JCGM 100(JCGM 2008) is following in this research work. The maximum uncertainty values for the measuring equipment's are mentioned in the Table 1. These maximum uncertainties are obtained from accuracy of

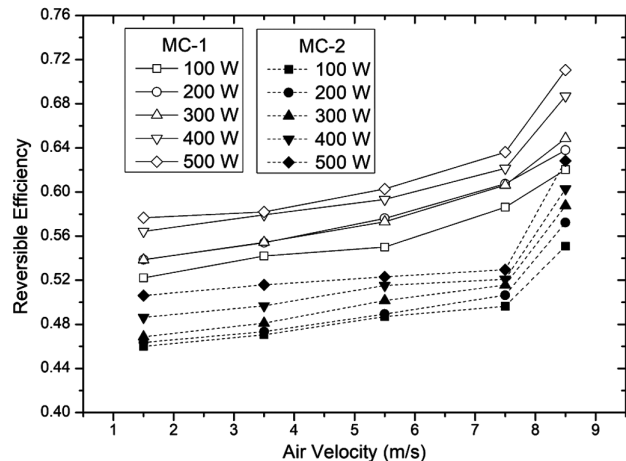


Fig. 8 — Reversible efficiency variation under several air velocities and heat inputs for $T_a = 50^\circ\text{C}$, and $n=6500$.

Table 3 — Relative uncertainty for the performance parameters.

Parameter	Relative uncertainty	Propagate uncertainty expression
Cooling capacity (W)	2.7%	$\sqrt{((h_1 - h_2) \cdot \delta M_R)^2 + (M_R \cdot \delta h_1)^2 + ((-1)M_R \cdot \delta h_2)^2}$
Compressor work or power consumption by the compressor (W)	3.8%	$\sqrt{((h_2 - h_1) \cdot \delta M_R)^2 + (M_R \cdot \delta h_2)^2 + ((-1)M_R \cdot \delta h_1)^2}$
Coefficient of performance (COP)	4.7%	$\sqrt{\left(\left(\frac{1}{W_{in}}\right) \cdot \delta Q_E\right)^2 + \left(-\left(\frac{Q_E}{W_{in}}\right) \cdot \delta W_{in}\right)^2}$
Reversible COP	0.43%	$\sqrt{((-1) \cdot \delta T_C)^2 + (1 \cdot \delta T_E)^2}$
Relative efficiency	4.7%	$\sqrt{\left(\left(\frac{1}{COP_{rev}}\right) \cdot \delta(COP)\right)^2 + \left(-\left(\frac{COP}{COP_{rev}}\right) \cdot \delta(COP_{rev})\right)^2}$
Condenser heat rejection rate (W)	3.24%	$\sqrt{((h_2 - h_3) \cdot \delta M_R)^2 + (M_R \cdot \delta h_2)^2 + ((-1)M_R \cdot \delta h_3)^2}$

the measuring devices for the confident level of 95% and the mass flow meter, refrigerant temperature and pressure sensor are used to measure the mass flow rate of the refrigerant, refrigerant temperature at specific location and refrigerant pressure at the specified point. Table 3 reports the uncertainty values for the performance parameters used in this work. These performance parameters are calculated using enthalpy entering and leaving from the condenser and evaporator respectively. These enthalpy values are taken from the Refrigerant table data book with corresponding refrigerant pressure and temperature values. The uncertainty values for these data book values are considered as 0.5% of end value³⁹. The uncertainty values for all the performance parameters are having low values and it is lesser than 5%. So, it can be concluded that the experimental setup facility and equipment's are worked properly and efficiently.

3.3 Personal cooling system integration

Following the performance testing of the miniature VCR-based personal cooling system with two distinct microchannel condensers, a prototype personal cooling jacket is proposed for development. The above section conclude that based on the weight, size, and performance, the MCC-2 condenser is proposed to develop the PCS. As a result, a prototype PCS is presented for development employing a miniature rotary compressor, microchannel condenser (MCC-2), a capillary tube (ID 1.18 mm), a flexible polyurethane tube, a fireman jacket, and a battery. The entire weight of the PCS is 4.335 kg, including the battery and jacket. The firefighter's jacket is made up of three layers. These are the exterior, middle, and interior

layers. The outer layer protects against flashovers. It is constructed of a flame-retardant fabric that is woven of 93% metaramide, 5% paraaramide, and 2% anti-static material. The middle layer serves as a moisture barrier, allowing perspiration and heat to escape to the outside environment, minimizing heat stress and protecting the wearer from water penetration. The inner layer is a heat barrier made of nonwoven aramid fibers like Nomex or Kevlar. Overall, this jacket weights 1.62 kg.

A 24 V 10.5 Ah lithium-ion battery weighing 600 g and lasting three hours is employed. The rotary compressor is placed at the left bottom side (front) of the jacket and condenser is fitted at the right bottom (front) of the jacket. The battery is placed at the side of the human body. Three pockets are stitched in the outer layer of the jacket and These three devices are placed inside the pockets. The sufficient air flow is maintained in all three pockets for removing the heat from the devices. The flexible evaporator tube stitched in the inner layer of the jacket and it will be touched at the human skin for absorbing the heat from human body. Each component's weight is listed in Table 4. This table clearly shows that the present work is having lesser than compared to Yuan²⁷ and Ernst and Garimella²⁵. But, vest weight consumes the 37% of the total system weight. Because firefighters required the more protection from the thermal environment. In the other researcher work, Morriesen *et al.* (2012)²³, Wu *et al.* (2010)²² and Elbel *et al.* (2012)²⁴ did not mentioned the vest and power source weight clearly. But, present work system weight is better than others.

Table 4 — The weight of each component of the small VCR-based PCS.

Component	Weight in kg					
	Present work	Yuan <i>et al.</i> (2015)	Ernst and Garimella (2013)	Morriesen <i>et al.</i> (2012)	Wu <i>et al.</i> (2010)	Elbel <i>et al.</i> (2012)
Compressor	0.925	0.590	0.44	1.17	0.4	--
Condenser	0.4	0.38	1.22	0.16	0.26	--
Expansion valve	0.06	0.14	0.10	--	--	--
Evaporator	0.13	0.265	0.53	--	0.3	--
Jacket	1.62	--	0.32	--	--	--
Battery	1.2	--	1.57	--	--	1.5
Total	4.335	5.25	5.31	3.5*	2.85*	2.25*

* Not including vest weight

4 Conclusion

Miniature VCR-based PCS performance is evaluated using two dissimilar microchannel condensers (MCC-1 and MCC-2) with an effect of air velocity (range: 1.5–8.5 m/s) for moderate firefighters' working conditions ($T_a = 50^\circ\text{C}$ and body heat generation range = 100–500 W). The following conclusions are made from this study.

- The suction pressure decreases with an increase in air velocity and increases with a rise in heat input. The suction pressure of MCC-2 is more than that of MCC-1 in all heat inputs due to improper two-phase heat transfer performance (condensation of the refrigerant) when the air velocity decreases.
- When decreasing the air velocity, the suction pressure of MCC-1 is increased by 8.57% and 6.4% for 100 W and 500 W respectively. However, MCC-2 is increased by 6.6% and 6.4% for 100 W and 500 W respectively.
- The cooling load capacity, COP, and the reversible efficiency rise with an rise in air velocities and heat inputs.
- Based on the cooling load capacity and COP, MCC-1 and MCC-2 performed similarly at maximum air velocity. Because the change in cooling load capacity and COP of MCC-1 and MCC-2 is less than 3.2% only.
- At maximum air velocity (8.5 m/s), the increase in reversible efficiency of MCC-1 is 12.62% and 13.1% higher than that of MCC-2 for 100 W and 500 W correspondingly.
- Based on the weight, size, and performance, the MCC-2 condenser is proposed to develop the PCS.
- The proposed PCS for firefighters in moderate working circumstances weighs 4.335 kg, including the battery, and can run for three hours.
- In the future, rather than employing an Aspen rotary compressor, the linear compressor will be

developed. Because the linear compressor has the advantage of being able to work at any orientation or angle.

Acknowledgment

The Department of Science and Technology supports financially through the scheme of the Instrumentation Development Programme (F. No: IDP/IND/11/2015).

References

- Hemmatjo R, Motamedzade M & Aliabadi M, *Health Promot Perspect*, 7 (2017) 66.
- Barr D, Gregson W & Reilly T, *Appl Ergon*, 41 (2010) 161.
- Rossi R, *Ergon*, 46 (2003) 1017.
- Taylor NA, *Ind Health*, 44 (2006) 331.
- Gutierrez-Arroyo J, Rodriguez-Marroyo J A & Garcia-Heras F, *Front Public Health*, 12 (2024) 1408591.
- Deng Q, Zhao J & Liu W, *Build Environ*, 137 (2018) 17.
- Smith D L, S MT & Petruzzello S J, *Ergon*, 44 (2001) 244.
- Xu Y, Li Z & Wang J, *Appl Thermal Eng*, 200 (2022) 117730.
- Zhang H & Song G, *J Industrial Textiles*, 44 (2013) 288.
- Mokhtari Yazdi M & Sheikhzadeh M, *The J Textile Institute*, 105 (2014) 1231.
- Nunneley SA, *Space Life Sci*, 2 (1970) 335.
- Sajjad U, Hamid K & Tauseef U R, *Int Comm Heat Mass Transf*, 130 (2022) 105739.
- Weicheng S, Wang J, Zhang X, *J Electronic Packaging*, 142 (2020) 1.
- Fu R P, Qu Z G & Tao W Q, *Appl Thermal Eng*, 194 (2021) 117107.
- Heydari A, *ITherm 2002 Eighth Intersociety Conference on Thermal and Thermomechanical Phenomena in Electronic Systems (Cat No02CH37258)*, (2002) 371.
- Trutassanawin S, Groll E A & Garimella S V, *IEEE Transac Compon Packa Technol*, 29 (2006) 678.
- Yang Y F, Yuan W X & Liao Y B, *Appl Mech Mater*, 321 (2013) 383.
- Lee J & Mudawar I, *J Electronic Packa*, 128 (2005) 30.
- Bentrcia M, Alshatewi M & Omar H, *Adv Mech Eng*, 9 (2017) 1.
- Kumar S S & Kumaraguruparan G, *J Brazilian Soc Mech Sci Eng*, 45 (2023) 422.

- 21 Grzyll L R & McLaughlin T, *IECEC-97 Proc Thirty-Second Intersoc Energy Convers Eng Conf (Cat No97CH6203)* 27 July-1 Aug. 1997 1997, pp.1624-1629 vol.1623.
- 22 Wu Y T, Ma F & Zhong X H, *Energy Conver Manage*, 51 (2010) 81.
- 23 Ribeiro G, Morriesen A & Resende F, *Purdue Int Refrige Air Conditioning Conf* (2012).
- 24 Elbel S, Bowers C D & Zhao H, *Purdue Int Refrige Air Conditioning Conf* (2012).
- 25 Ernst T C & Garimella S, *Appl Thermal Eng*, 60 (2013) 316.
- 26 Guo T, Shang B & Duan B, *J Therm Biol*, 49 (2015) 47.
- 27 Yuan W, Yang B & Yang Y, *Appl Energy*, 143 (2015) 47.
- 28 Bartkowiak G, Dabrowska A & Marszalek A, *Appl Ergon*, 58 (2017) 182.
- 29 Lee W J & Jeong J H, *Int J Refrige*, 69 (2016) 85.
- 30 Yang L J, Du X Z & Yang Y P, *Int J Heat Mass Transf*, 54 (2011) 3109.
- 31 Dodiya K, Bhatt N & Lai F, *Int J Ambient Energy*, 43 (2020) 1.
- 32 Veerabhadrapa Bidari M, B NP & Lalagi G, *Int J Ambient Energy*, 43 (2022) 5718.
- 33 Meikandan M, *Int J Ambient Energy*, 41 (2020) 500.
- 34 Lee T S, Wu W C & Chuah Y K, *Int J Refrige*, 33 (2010) 1370.
- 35 Li J, Gao Y & Liu C, *Int Comm Heat Mass Transf*, 149 (2023) 107135.
- 36 Oh S H, Lee S H & Lee D, *Int J Heat Mass Transf*, 176 (2021) 121460.
- 37 Yumrutaş R, Kunduz M & Kanoğlu, *Exergy, An Int J*, 2 (2002) 266.
- 38 Ahamed J U, Saidur R & Masjuki H H, *Renew Sustain Energy Rev*, 15 (2011) 1593.
- 39 Illán-Gómez F, García-Cascales J & Hidalgo-Mompeán F, *Energy Build*, 144 (2017) 104.